



Cite this: RSC Adv., 2021, 11, 38774

# Effective screen-printed potentiometric devices modified with carbon nanotubes for the detection of chlorogenic acid: application to food quality monitoring

Hisham S. M. Abd-Rabboh,<sup>ab</sup> Abd El-Galil E. Amr,<sup>acd</sup> Ahmed M. Naglah,<sup>c</sup> Abdulrahman A. Almehezia<sup>c</sup> and Ayman H. Kamel<sup>be</sup>

All-solid state screen-printed electrodes were fabricated for chlorogenic acid (CGA) detection. The screen-printed platforms were modified with multi-walled carbon nanotubes (MWCNTs) to work as a lipophilic solid-contact transducer. The sensing-membrane was plasticized with a suitable solvent mediator and incorporating  $[\text{Ni}^{\text{II}}(\text{bathophenanthroline})_3][\text{CGA}]_2$  complex as a sensory material. In a 30 mM phosphate solution (buffer, pH 6), the sensor revealed a Nernstian-response towards CGA ions with a slope of  $-55.1 \pm 1.1$  ( $r^2 = 0.9997$ ) over the linear range  $1.0 \times 10^{-7}$  to  $1.0 \times 10^{-3}$  ( $0.035\text{--}354.31 \mu\text{g mL}^{-1}$ ) with a detection limit  $7.0 \times 10^{-8}$  M ( $24.8 \text{ ng mL}^{-1}$ ). It revealed a stable potentiometric response with excellent reproducibility and enhanced selectivity over several common ions. Short-term potential stability and the interfacial sensor capacitance was estimated using both electrochemical-impedance spectroscopy (EIS) and chronopotentiometry techniques. The presented electrochemical platform revealed the merits of design simplicity, ease of miniaturization, good potential-stability, and cost-effectiveness. It is successfully applied to CGA determination in different coffee beans extracts and juice samples. The data obtained were compared with those obtained by liquid chromatography reference method (HPLC).

Received 7th November 2021  
Accepted 23rd November 2021

DOI: 10.1039/d1ra08152g

rsc.li/rsc-advances

## 1. Introduction

Chlorogenic acid (CGA), [5-O-caffeoylquinic acid], is naturally found in different plants such as *Calendula officinalis*, honey-suckle, *Eucommia* and *Echinacea purpurea*. It is produced by plants during aerobic respiration. It is classified as a phenyl-propanoid compound. This compound has a very wide range of biological activities.<sup>1</sup> It serves as anti-hypertension,<sup>2</sup> anti-inflammatory,<sup>3</sup> anti-carcinogenic,<sup>4</sup> anti-bacterium<sup>5</sup> and anti-tumor agent.<sup>6</sup> Furthermore, there are also reports that CGA has a potential role in regulating blood glucose in type 2 diabetes, increasing white blood cells. In addition, it lowers blood-lipids, scavenges free-radicals, and excites central-nervous system.<sup>7–9</sup> Therefore, quantitative assessment of CGA in plants has merited great interest. There are various analytical methods have

been reported for CGA quantification. These methods include liquid chromatography,<sup>10–14</sup> thin-layer scanning,<sup>15</sup> capillary electrophoresis,<sup>16–18</sup> fluorescence spectrometry,<sup>19</sup> infrared spectroscopy,<sup>20</sup> and electrochemical methods.<sup>21–32</sup> One of the most promising electrochemical techniques is potentiometric based sensors. In the local markets, there are various conventional-potentiometric sensors were commercially available. In addition, there are many potentiometric sensors were reported in the literature for sensitive and selective monitoring of various ions in different application-fields.<sup>33–44</sup> A biomimetic potentiometric sensor was developed for CGA based on molecularly imprinted polypyrrole (MIPpy) on pencil-graphite substrate.<sup>45</sup>

Screen-printed electrodes (SPEs) are now widely used to improve the development and characterization of new electroanalytical methods.<sup>46</sup> They are characterized by their large-scale production, ease-of-use, portability, and reduced costs for analysis.<sup>47</sup> In addition, they have high reproducibility that make them suitable for a wide range of applications, such as clinical, environmental and food industry analysis.<sup>35–37,48</sup> Surface modification of these types of platforms have received great attention allowing their employment in a variety of sensors and biosensors.<sup>49–51</sup> Recently, screen-printed sensors have received great attention. To increase the potential stability and reliability of these types of electrodes, different nanomaterials with excellent electrochemical features have been utilized as solid-contact transducers.

<sup>a</sup>Chemistry Department, Faculty of Science, King Khalid University, Abha 61413, Saudi Arabia

<sup>b</sup>Department of Chemistry, Faculty of Science, Ain Shams University, Cairo 11566, Egypt. E-mail: ahkamel76@sci.asu.edu.eg; ahmohamed@uob.edu.bh

<sup>c</sup>Pharmaceutical Chemistry Department, Drug Exploration and Development Chair (DEDC), College of Pharmacy, King Saud University, Riyadh 11451, Saudi Arabia. E-mail: aamr@ksu.edu.sa

<sup>d</sup>Applied Organic Chemistry Department, National Research Center, 12622 Dokki, Giza, Egypt

<sup>e</sup>Chemistry Department, College of Science, Sakheer 32038, Kingdom of Bahrain


In this work, a novel potentiometric screen-printed sensor modified with multi-walled carbon nanotubes (MWCNTs) was fabricated for chlorogenic acid determination. Experimental parameters of the analytical procedure such as sensitivity, selectivity, pH effect, short-term potential stability and lifespan were optimized. The presented sensor was introduced successfully for the assessment of CGA in green-coffee beans extracts and fruit-juice samples.

## 2. Experimental

### 2.1 Chemicals and reagents

Chlorogenic acid (CGA), quinic acid, caffeic acid, acetic acid, potassium chloride, 4,7-diphenyl-1,10-phenanthroline (bphen) ( $\geq 97\%$  purity), high molecular weight poly(vinyl chloride) (PVC), 2-nitrophenyl octyl ether (*o*-NPOE) and nickel ammonium sulfate and tetrahydrofuran were purchased from Sigma-Aldrich (St. Louis, MO, USA). Tetradodecyl-ammonium tetrakis(4-chlorophenyl)borate (ETH500) was purchased from Fluka AG (Buchs, Switzerland). MWCNTs were purchased from (EPRI, Cairo, Egypt). Ag/AgCl ink (E2414) was purchased from Ercon (Wareham, MA). Milli-Q PLUS reagent-grade water system (Millipore) was used for obtaining de-ionized water with a specific resistance 18.2 M $\Omega$  cm.

Phosphate buffer solution was prepared from a mixture of Na<sub>2</sub>HPO<sub>4</sub>·2H<sub>2</sub>O and NaH<sub>2</sub>PO<sub>4</sub>·2H<sub>2</sub>O with all components at concentration of 30 mM and pH value of 6.0. CGA solutions were freshly prepared in hot water daily and stored in brown bottles at 4 °C when not in use. All potentiometric measurements were carried out in 30 mM phosphate buffer solution, pH 6.

### 2.2 Apparatus

All measurements were carried out using mV/pH meter (PXSJ-216, INESA, Scientific Instrument Co., Ltd, Shanghai, China). Modified screen-printed platforms with carbon screen (SPEs) were purchased from DropSens (LLanera, Asturias, Spain). The platforms were modified with multi-walled carbon nanotubes (MWCNTs) (ref. 110CNT) which were made from ceramic ( $L$  34  $\times$   $W$  10  $\times$   $H$  0.5 mm) and silver as an electrical contact. For chronopotentiometry measurements, they were carried out using potentiostat/galvanostat (Autolab 204, Metrohm, Herisau, Switzerland). A classical three-electrode cell of volume 10 mL was used with a CGA working electrode, a platinum wire ( $\varnothing$ : 3 mm, diameter) auxiliary electrode and an Ag/AgCl (3 M KCl) reference electrode (Orion 90-02, USA).

### 2.3 Preparation of the ion association nickel<sup>II</sup>-bathophenanthroline/CGA complex

A 0.1 g of 4,7-diphenyl-1,10-phenanthroline (bphen) was dissolved in 20 mL of ethyl alcohol and then a 3 mL of 0.1 M NiSO<sub>4</sub> solution was added. The solution was then mixed with 10 mL of 0.1 M CGA solution (pH, 6), and stirred for 5 min. A pale green precipitate of Ni<sup>II</sup>-bathophenanthroline/CGA [Ni<sup>II</sup>(bphen)<sub>3</sub>][CGA]<sub>2</sub> was produced. The precipitate was isolated from the mother liquor and washed several times with de-ionized water. The precipitate was dried at room temperature, and grinded to

a fine powder. The obtained precipitate was analyzed using C,H,N elemental analyzer. Nickel content in the precipitate was analyzed using atomic absorption spectrometry (AAS).

### 2.4 Sensors' construction

The sensing-membrane cocktail was prepared by dissolving 100 mg of the membrane components in 2 mL THF solvent: [Ni<sup>II</sup>(bphen)<sub>3</sub>][CGA]<sub>2</sub> (2 wt%), *o*-NPOE (49 wt%), ETH500 (1 wt%) and PVC (48 wt%). The SPE platforms were sonicated in water for 10 min, washed with de-ionized water and then washed with ethanol and left to dry. To the modified carbon screen in the SPE platform, a 15  $\mu$ L of the sensing-membrane solution was drop-casted to prepare the working electrode. The membrane was left to dry for 6 hours. To the same SPE platform, the Ag/AgCl screen is coated with a layer of Ag/AgCl ink, and then it was left to dry. The reference electrode (Ag/AgCl) was prepared by adding 10  $\mu$ L of the reference-membrane solution on the Ag/AgCl ink electrode surface. This reference membrane was prepared after dissolving 70 mg of NaCl and 78.1 mg of polyvinyl butyral (PVB) in 1 mL of methanol.<sup>52</sup>

### 2.5 Electrochemical characterization of the SPE sensors

The interfacial capacitance of the presented SPEs and membrane bulk resistance were evaluated using both chronopotentiometric and impedance measurements, respectively. A classical three-electrode cell of volume 10 mL was used for performing these measurements. The working SPE sensor in conjunction with the reference electrode the auxiliary Pt electrode were immersed in 10<sup>-3</sup> M CGA solution. In the chronopotentiometry, a constant current of  $\pm 1$  nA was applied onto the working electrode for fixed time-interval (60 s) and then followed by a reversed-current for another 60 s. In impedance spectroscopy measurements, the applied-frequency range was 100 kHz to 0.1 Hz. A sinusoidal-excitation signal with an excitation amplitude of 10 mV was used.

### 2.6 Analysis of real samples

The sensors were applied for the analysis of CGA in different green coffee extracts and fruit juice samples. For the green coffee samples, 0.2 g of sample was inserted in a 50 mL beaker containing 10 mL acetic acid (1%, v/v). The mixture was stirred under ultrasonic extractor for 2 h. The extract was then centrifuged, decanted, and the residue was re-extracted with the same solvent. After centrifugation, the filtrates were kept in the refrigerator at 4 °C. Prior to the analysis, the extracts were diluted to 25 mL of 30 mM phosphate buffer (pH 6.0). For fruit juice samples, they were directly diluted with the buffer solution, then subjected to the analysis.

## 3. Results and discussion

### 3.1 Sensor's performances and characteristics

All-solid state modified screen-printed (SPEs) potentiometric sensors were fabricated, characterized, and introduced as sensors for chlorogenic acid detection (Fig. 1).



The membrane sensors were plasticized with a suitable solvent mediator and incorporating  $[\text{Ni}(\text{bphen})_3][\text{CGA}]_2$  complex as a sensory material. CGA anion reacts with  $[\text{Ni}(\text{bphen})_3]^{2+}$  cation to form 1 : 2  $[\text{Ni}(\text{bphen})_3][\text{CGA}]_2$  ion-pair complex. The stoichiometric ratio between  $[\text{Ni}(\text{bphen})_3]^{2+}$  cation and CGA anion chemical was confirmed by the elemental analysis. The calculated values were, (C: 59.626%, H: 4.04%, N: 4.01%, and Ni: 2.801%; found, C: 58.954%, H: 4.01%, N: 4.103 and Ni: 2.782%). The composition of the membrane for the proposed SPE was 2 : 1 : 49 : 48% (w/w) ion-pair complex; ETH500; *o*-NPOE plasticizer and PVC, respectively. The potentiometric response for all-solid-state SPEs were evaluated and tested in the concentrations range of  $1.0 \times 10^{-2}$  to  $1.0 \times 10^{-8}$  M CGA solutions in 30 mM phosphate buffer solution, pH 6. The dynamic time-trace for the potential response with its corresponding calibration plot were shown in Fig. 2. The sensors exhibited a Nernstian-response with a slope of  $-55.1 \pm 1.1$  mV per decade ( $r^2 = 0.9997$ ) over the linear range ( $1.0 \times 10^{-7}$  to  $1.0 \times 10^{-3}$  M) and low detection limit of  $7 \times 10^{-8}$  M ( $24.8 \text{ ng mL}^{-1}$ ).

The time-trace of the presented sensor was evaluated by measuring the potential after varying the concentration of CGA

over an interval time 2 min. The time taken to reach equilibrium was found to be <5 seconds. The response was reversible, decreasing immediately and recovering its baseline when the electrode was placed again in the buffer solution. This confirms the reversibility of binding CGA molecule with the  $[\text{Ni}(\text{bphen})_3][\text{CGA}]_2$  ion-pair complex.

The effect of pH of the test solutions on the sensor's response was also examined over different pH solutions. The sensor revealed a stable potential for two CGA concentrations (e.g.  $10^{-4}$  and  $10^{-3}$  M) over the pH range 4 to 8. At pH < 4, the response was declined due to the formation of the non-ionized CGA molecule. The  $\text{pK}_a$  values of CGA were 3.33, 8.5 and 12.75 for carboxylic and di-phenolic groups, respectively.<sup>53</sup> At pH > 8.5, the slope of the sensor declined due to the formation of the di-valent CGA.

### 3.2 Transduction mechanism

For all potentiometric ion-selective electrodes based on solid-contact transducers without redox properties, the ion-to-electron transduction is based on the formation of electrical

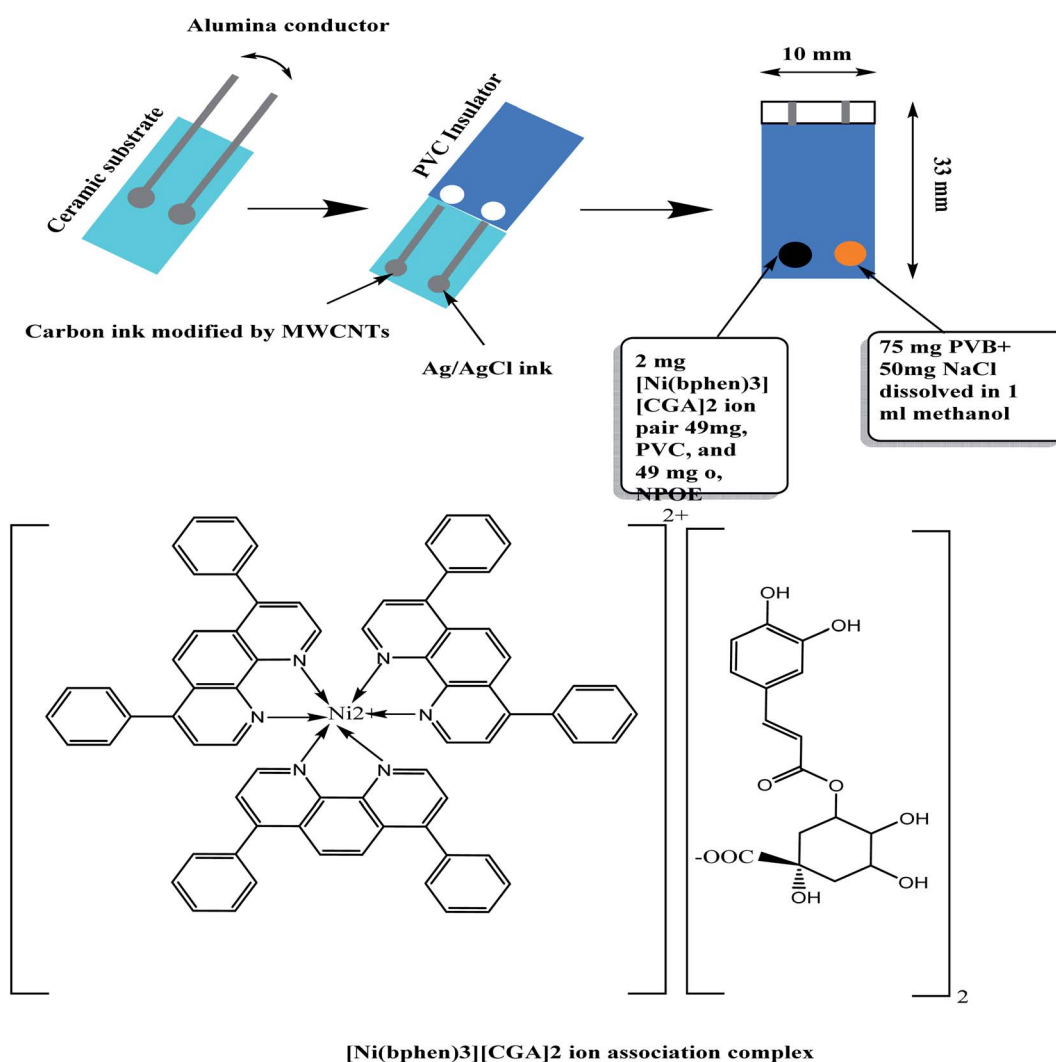


Fig. 1 Schematic representation of the presented sensors.



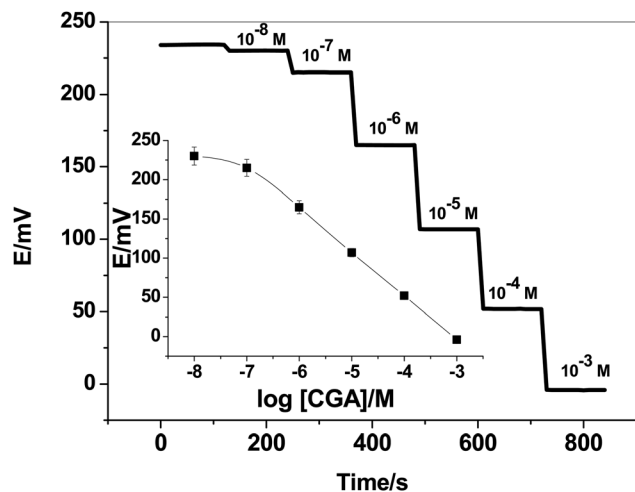


Fig. 2 Time-trace of the presented CGA-ion-selective electrode. The inset shows the calibration plot of the sensor.

double layer between the sensor's membrane and the solid-contact interface as shown in Fig. 3. This interface can work as an asymmetrical electrical capacitor. One side carries charge in the form of CGA ions coming from the ion-selective membrane, and the other side is formed by holes in the solid-contact MWCNTs layer. The interfacial potential at the ISE membrane/solid contact interface defined by the quantity of these charges in the electrical double-layer. It is neither defined by ion-partitioning between two phases nor by a redox reaction. The presence of MWCNTs layer prevents the formation of the un-desired aqueous layer between the sensor's membrane and the underlying conducting substrate. This provides a potential stability for the sensor and prevents its potential-drift. MWCNTs as one of the carbons nanomaterials are

characterized by their chemical stability under potentiometric conditions and exhibited high specific surface areas due to their unique nanostructures.

### 3.3 Analytical method validation

**3.3.1 Linearity range and detection limit.** Sensor's performance characteristics revealed a linear-dynamic range between  $1.0 \times 10^{-7}$  to  $1.0 \times 10^{-3}$  M with near-Nernstian slopes of  $-55.1 \pm 1.1$  mV per decade. The regression equation of the calibration plot was  $Y \text{ (mV)} = -55.1 \log x - 351.2$  with a correlation coefficient of  $r^2 = 0.9997$  between the standard CGA concentration ( $x$ ) and the potential measured in triplicates.

The detection limit (DL) was evaluated as the concentration corresponding to the intersection of the extrapolated linear segment of the calibration graph. The DL was found to be  $24.8 \text{ ng mL}^{-1}$ .

**3.3.2 Repeatability, reproducibility, and stability.** The design of screen-printed sensors involves simple operational steps which facilitate the mass-production of devices with similar analytical-performance. The repeatability of the presented platforms was excellent for the electrode process of CGA as an RSD of 1.2% for different calibration plots ( $n = 10$ ). Reproducibility of the designed sensor was examined by constructing the calibration curves of different prepared sensors ( $n = 5$ ) under the same experimental conditions of measurements. The relative standard deviation (RSD) showed a reproducibility of 2.2%. These values showed an accepted repeatability and reproducibility of the presented sensor platform. The presented sensor revealed high potential-stability and retained its analytical performances over a period and repeated usage. The potential-stability was tested after measuring 10 mM and 0.1 mM CGA solutions for 2 weeks continuously. The slopes of the constructed calibration plots were calculated every day over

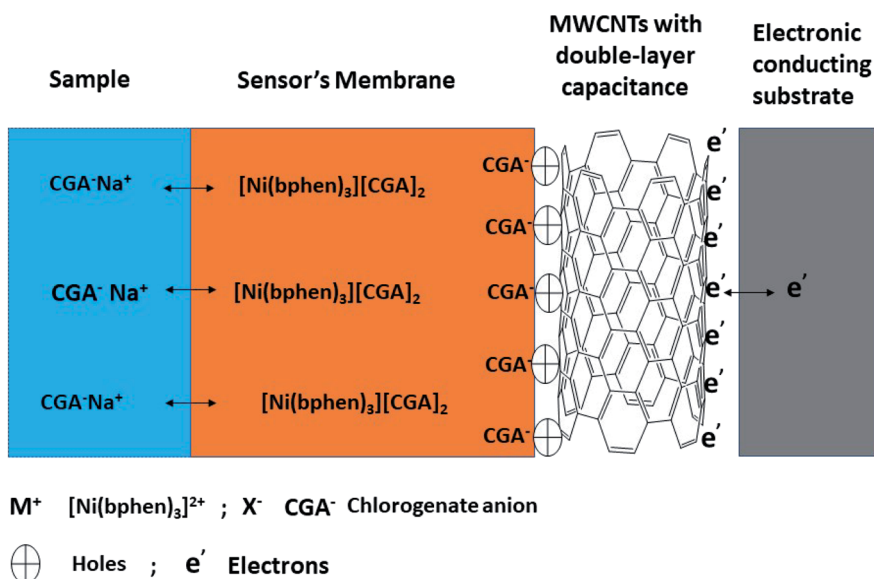


Fig. 3 Schematic representation of all relevant interfaces within CGA sensor contains an ion-exchanger sensing material ( $[\text{Ni}(\text{bphen})_3][\text{CGA}]_2$ ). The sensor is based on a high-surface-area SC (i.e. MWCNTs) exhibiting a high double layer capacitance.



these two weeks ( $n = 3$ ). The slope variation was found to be  $<1.3$  mV per decade after 10 working days.

**3.3.3 Method accuracy.** The method accuracy was evaluated by measuring a spiked known amount of the standard CGA solution. Each sample was analyzed in triplicate ( $n = 3$ ). The obtained accuracy was found to be 99.1–103.1%.

### 3.4 Sensors' selectivity

Selectivity of the presented sensor is an essential parameter for evaluating its selectivity-behavior towards CGA ion over other tested interfering ions. In addition, it determines the successful applicability in real samples with different matrices. Selectivity and its coefficient values ( $K_{CGA,J}^{pot}$ ) were examined and calculated using the modified separate solutions method (MSSM).<sup>54</sup> The selectivity coefficient values for all these tested interfering ions were presented in Table 1. The selectivity order was in the order: CGA  $\gg$  quinic acid  $>$  ferulic acid  $>$  vanillic acid  $>$  caffeic acid  $>$  ascorbic acid  $>$  chloride  $>$   $SO_4^{2-}$   $>$   $CH_3COO^-$ . The obtained results showed high selectivity towards CGA over other compounds such as quinic and ferulic which had molecular structures like CGA.

### 3.5 Chronopotentiometry and impedance measurements

Short-term potential stability for the presented electrode was evaluated using chronopotentiometric measurements.<sup>55</sup> This approach has become the best method for the evaluation of the short-term potential stabilities of all-solid-state ion-selective sensors. It implies the application of  $\pm 1$  nA of direct current on the electrode and the potential is then recorded. The test solution was 10 mM of CGA solution. The potential drift of either modified or non-modified screen-printed electrode was calculated from the slope ( $\Delta E/\Delta t$ ) of the potential/time plot. It was found the potential drift of both the modified and non-modified screen-printed platforms was  $34.5$  and  $134 \mu V s^{-1}$ , respectively. The chronopotentiograms for modified and non-modified CGA sensors were shown in Fig. 4. These obtained data showed the potential-stability enhancement of the presented sensor after the insertion of MWCNTs layer between the electronic conductor substrate and the ion-sensing membrane and its successful application of this nanomaterial as a solid-contact transducer. The double-layer capacitances ( $C_L$ ) for both modified and non-modified screen-printed CGA sensors were found to be  $29.2 \pm 1.2$  and  $7.4 \pm 1.2 \mu F$ , respectively.

Impedance spectroscopy measurements were applied on both the modified and non-modified CGA sensors. The typical impedance spectra of the presented electrodes were shown in

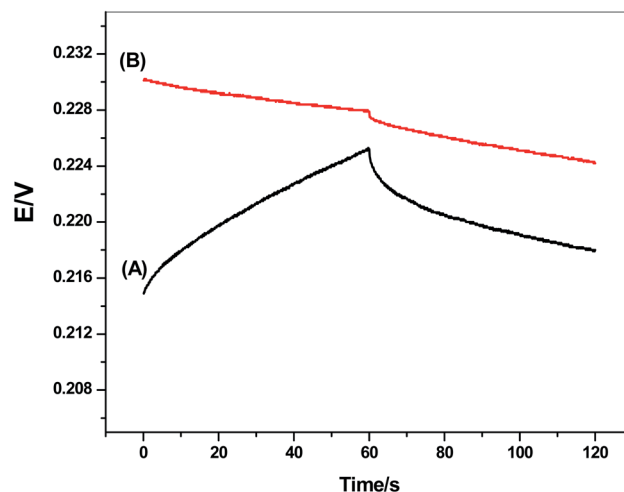


Fig. 4 Chronopotentiograms for (A) non-modified and (B) modified CGA sensor under the constant currents of  $\pm 1$  nA in  $1.0 \times 10^{-3}$  M solution.

Fig. 5. The resistance of the membrane ( $R_b$ ) was calculated from the high-frequency semi-circle. It was found that the resistances ( $R_b$ ) of the non-modified and modified screen-printed sensors were  $7.68 \pm 0.6$  and  $9.1 \pm 0.3$  k $\Omega$ , respectively. From the low-frequency semicircle, the double-layer capacitances ( $C_L$ ) of the non-modified and modified screen-printed sensors were found to be  $10.3 \pm 0.5$  and  $31.8 \pm 0.4 \mu F$ , respectively. These results confirmed that the existence of the MWCNTs layer as solid-contact transducer is significantly affect on the rate of charge transportation between the interfaces. In addition, it offers a high-potential stability for the presented CGA solid-contact ion-selective electrode.

### 3.6 Water-layer test

Water-layer formation between the ion-sensing membrane and the electronic conductor substrate is responsible for the potential-drift of the sensors. To test the water-layer formation, the screen-printed platforms electrodes in presence/absence of MWCNTs layer were initially inserted in 0.1 M NaCl solution as a discriminating ion for 6 h. After, the solution was changed to the CGA ion solution ( $10^{-4}$  M). After 6 h, the CGA ion solution was replaced by 0.1 M NaCl solution, and the potential was recorded for 12 h. The potential–time plot was constructed and shown in Fig. 6. The modified CGA electrode showed very stable potential upon replacing the primary ions by the discriminated ions while the non-modified electrode revealed a significant

Table 1 Potentiometric selectivity coefficient  $\log K_{CGA,J}^{pot}$  for the presented CGA sensor

Sensor type	Caffeic acid	Ascorbic acid	Ferulic acid	Vanillic acid	Quinic acid	$Cl^-$	$SO_4^{2-}$	$CH_3COO^-$
This work	$-3.5 \pm 0.4$	$-4.5 \pm 0.3$	$-3.1 \pm 0.7$	$-3.4 \pm 0.2$	$-2.4 \pm 0.5$	$-5.6 \pm 0.3$	$-5.7 \pm 0.1$	$-5.9 \pm 0.2$

<sup>a</sup> Average of three measurements.



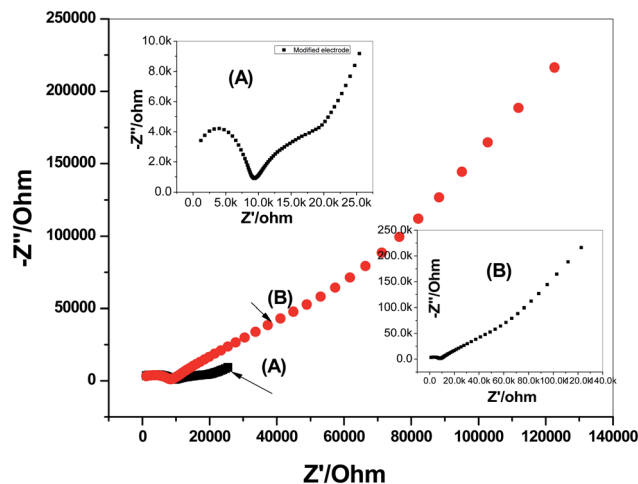


Fig. 5 Electrochemical impedance spectroscopy (EIS) measurements of: (A) modified and (B) non-modified CGA membrane-based sensors.

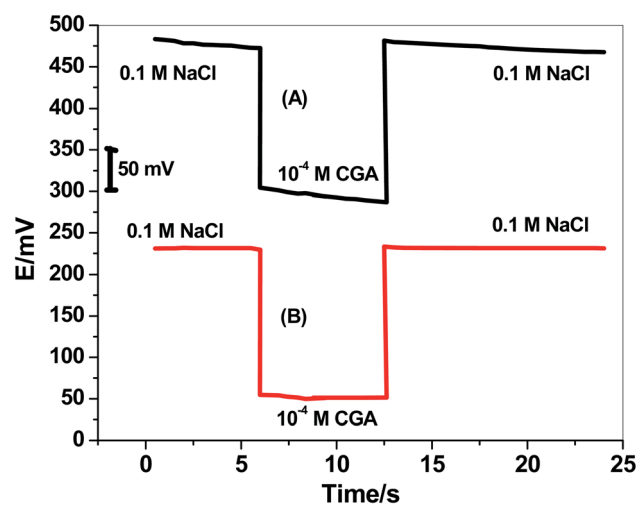


Fig. 6 Water-layer test for CGA membrane sensors (A) with and (B) without MWCNTs.

potential drift. This confirmed that the presence of the hydrophobic solid-contact material between the ion-sensing membrane and electronic conducting substrate prevents the formation of the water-layer, and a stable potential reading for the electrode platform is obtained.

### 3.7 Analytical applications

The presented sensor was successfully applied for the assessment of CGA in real samples with different matrices such as green coffee extracts and fruit juice samples. All CGA contents found in these real samples were presented in Table 2. The data were compared with those obtained by the reference liquid chromatography method (HPLC). The measurements were obtained with reasonable values of relative standard deviations (RSDs). Mean recoveries of 91.0% (RSD of 1.2%), 100.5 (RSD 1.1%) and 98.6% (RSD of 2.1%) were obtained on the spiked standard of three individual concentrations of CGA on the coffee bean extracts. For juice samples, the mean recoveries after spiking three standard CGA concentrations were 105.5% (RSD of 2.3%), 102.0 (RSD 0.9%) and 97.9% (RSD of 2.3%). The reasonable values of recoveries and RSDs calculated for the presented sensor revealed that method of analysis was accurate and precise for the assessment of CGA.

## 4. Conclusions

All-solid state screen-printed platforms modified with multi-walled carbon nanotubes (MWCNTs) was used for the sensitive and selective determination of chlorogenic acid (CGA). The membrane sensors were plasticized with a suitable solvent mediator and incorporating  $[\text{Ni}(\text{bphen})_3][\text{CGA}]_2$  complex as a sensory material. In a 30 mM phosphate buffer solution of pH 6, CGA is completely ionized and exists in the monovalent anion form, in which the presented sensor can detect it. The sensor revealed good analytical performance: near-Nernstian response for CGA ions with a slope of  $-55.1 \pm 1.1$  ( $r^2 = 0.9997$ ) mV per decade, detection limit of  $7.0 \times 10^{-8}$  ( $24.8 \text{ ng mL}^{-1}$ ), and linear concentration range of  $1.0 \times 10^{-7}$  to  $1.0 \times 10^{-3}$  M ( $0.035$ – $354.31 \text{ } \mu\text{g mL}^{-1}$ ). The presented sensor offered different merits, such as design simplicity, cost effectiveness, and short

Table 2 Assessment of CGA in different samples using the all-solid-state CGA sensor

Sample	CGA content					
	Potentiometric method					
	CGA	RSD%	Added ( $\mu\text{M}$ )	Found ( $\mu\text{M}$ )	Recovery (%)	HPLC method
Coffee bean extract 1	$19.2 \pm 1.3^a$	1.1	0.2	0.183	91.0	$18.8 \pm 0.3^a$
Coffee bean extract 2	$18.6 \pm 2.2^a$	1.3	0.4	0.402	100.5	$19.3 \pm 1.2^a$
Coffee bean extract 3	$21.3 \pm 1.7^a$	0.8	0.6	0.592	98.6	$20.8 \pm 0.2^a$
Tomato juice	$13.5 \pm 2.1^b$	1.2	0.2	0.211	105.5	$13.1 \pm 0.1^b$
Pomegranate juice	$12.1 \pm 1.4^b$	0.9	0.4	0.408	102.0	$12.5 \pm 0.2^b$
Black strawberry juice	$4.9 \pm 2.2^b$	1.3	0.6	0.587	97.8	$5.2 \pm 0.3^b$

<sup>a</sup> CGA in  $\text{mg g}^{-1}$ . <sup>b</sup> CGA in  $\text{mg per 100 mL}$ .

measuring time. The sensor was successfully introduced to CGA analysis in coffee bean extract samples and juices. Therefore, the obtained high sensitivity and selectivity towards CGA made the presented potentiometric method of high interest and a promising analytical tool for detecting CGA in food products.

## Author contributions

The listed authors contributed to this work as described in the following: H. S. M. A.-R., A. M. N., and A. H. K. gave the concepts of the work, interpretation of the results and prepared the manuscript. The experimental part was conducted by A. H. K. and H. S. M. A.-R. A. E.-G. E. A. cooperated in the preparation of the manuscript and A. H. K. and H. S. M. A.-R. performed the revision before submission. H. S. M. A.-R., A. A. A. and A. E.-G. E. A. revealed the financial support for the work. All authors have read and agreed to the published version of the manuscript.

## Conflicts of interest

The authors declare that there are no conflicts of interest. All authors have approved the manuscript and agree with the submission to your esteemed journal.

## Acknowledgements

H. S. M. A. extends his appreciation to the Deanship of Scientific Research at King Khalid University for funding this work through the Research Group Program under grant number RGP.1/286/42. The authors are grateful to the Deanship of Scientific Research, King Saud University for funding through Vice Deanship of Scientific Research Chairs.

## References

- X. H. Gu, R. Xu, G. L. Yuan, H. Lu, B. R. Gu and H. P. Xie, *Anal. Chim. Acta*, 2010, **675**, 64.
- I. J. Onakpoya, E. A. Spencer, M. J. Thompson and C. J. Heneghan, *J. Hum. Hypertens.*, 2015, **29**, 77.
- V. Francisco, G. Costa, A. Figueirinha, C. Marques, P. Pereira, B. Miguel Neves, M. Celeste Lopes, C. Rodríguez, M. Teresa Cruz and M. Teresa Batista, *J. Ethnopharmacol.*, 2013, **148**, 126.
- L. G. Naso, M. Valcarcel, M. Roura-Ferrer, D. Kortazar, C. Salado, L. Lezama, T. Rojo, A. C. González-Baró, P. A. M. Williams and E. G. Ferrer, *J. Inorg. Biochem.*, 2014, **135**, 86.
- Z. Lou, H. Wang, S. Zhu, C. Ma and Z. Wang, *J. Food Sci.*, 2011, **76**, 398.
- D. Wu, C. Bao, L. Li, M. Fu, D. Wang, J. Xie and X. Gong, *J. Pharmacol. Sci.*, 2015, **129**, 177.
- W. Y. Huang, Y. Z. Cai and Y. B. Zhang, *Nutr. Cancer*, 2010, **62**, 1.
- Y. Sato, S. Itagaki, T. Kurokawa, J. Ogura, M. Kobayashi, T. Hirano, M. Sugawara and K. Iseki, *Int. J. Pharm.*, 2011, **403**, 136.
- H. Hemmerle, H. J. Burger, P. Below, G. Schubert, R. Rippel, P. W. Schindler, E. Paulus and A. W. Herling, *J. Med. Chem.*, 1997, **40**, 137.
- A. P. Craig, C. Fields, N. Liang, D. Kitts and A. Erickson, *Talanta*, 2016, **154**, 481.
- C. M. Loescher, D. W. Morton, S. Razic and S. Agatonovic-Kustrin, *J. Pharm. Biomed. Anal.*, 2014, **98**, 52.
- A. K. Goey, H. Rosing, I. Meijerman, R. W. Sparidans, J. H. Schellens and J. H. Beijnen, *J. Chromatogr. B: Anal. Technol. Biomed. Life Sci.*, 2012, **902**, 151.
- R. Jaiswal, H. Müller, A. Müller, M. Gamaleldin, E. Karar and N. Kuhnert, *Phytochemistry*, 2014, **108**, 252.
- R. Jaiswal and N. Kuhnert, *J. Mass Spectrom.*, 2011, **46**, 269–281.
- V. Lebot, S. Michalet and L. Legendre, *J. Food Compos. Anal.*, 2016, **49**, 94.
- Z. Li, D. Huang, Z. Tang, C. Deng and X. Zhang, *Talanta*, 2010, **82**, 1181.
- E. Hurtado-Fernández, P. K. Contreras-Gutiérrez, L. Cuadros-Rodríguez, A. Carrasco-Pancorbo and A. Fernández-Gutiérrez, *Food Chem.*, 2013, **141**, 3492.
- N. B. Abu Bakar, A. Makahleh and B. Saad, *Anal. Chim. Acta*, 2012, **742**, 59.
- Q. Liu, Z. Dong, A. Hao, X. Guo and W. Dong, *Talanta*, 2021, **221**, 121372.
- A. Adnan, M. Naumann, D. Mörlein and E. Pawelzik, *Foods*, 2020, **9**, 788.
- Y. Yardım, E. Keskin and Z. Şentürk, *Talanta*, 2013, **116**, 1010.
- I. Vasilescu, S. A. V. Eremia, R. Penu, C. Albu, A. Radoi, S. C. Litescu and G. Radu, *RSC Adv.*, 2015, **5**, 261.
- M. Chao and X. Ma, *J. Food Drug Anal.*, 2014, **22**, 512.
- W. d. J. Rodrigues Santos, M. Santhiago, I. Valeria Pagotto Yoshida and L. T. Kubota, *Anal. Chim. Acta*, 2011, **695**, 44.
- T. Teker and M. Aslanoglu, *Arabian J. Chem.*, 2020, **13**, 5517.
- N. Mohammadi, M. Najafi and N. B. Adeg, *Sens. Actuators, B*, 2017, **243**, 838.
- I. Munteanu and C. Apetrei, *Int. J. Mol. Sci.*, 2021, **22**, 8897.
- S. C. Fernandes, S. K. Moccellini, C. W. Scheeren, P. Migowski, J. Dupont, M. Heller, G. A. Micke and I. C. Vieira, *Talanta*, 2009, **79**, 222.
- L. D. Mello, M. D. P. T. Sotomayor and L. T. Kubota, *Sens. Actuators, B*, 2003, **96**, 636.
- S. K. Moccellini, A. Spinelli and I. C. Vieira, *Enzyme Microb. Technol.*, 2008, **43**, 381.
- M. L. De Carvalho, M. Santhiago, R. A. Peralta, A. Neves, G. A. Micke and I. C. Vieira, *Talanta*, 2008, **77**, 394.
- W. D. R. Santos, M. Santhiago, I. V. P. Yoshida and L. T. Kubota, *Anal. Chim. Acta*, 2011, **695**, 44.
- N. H. Ashmawy, A. A. Almhizia, T. A. Youssef, E. A. A. El-Galil, M. A. Al-Omar and A. H. Kamel, *Molecules*, 2019, **24**, 1539.
- S. S. M. Hassan, E. M. Elnemma and A. H. K. Mohamed, *Electroanalysis*, 2005, **17**, 2246.
- A. H. Kamel, A. E. Amr, H. R. Galal, M. A. Al-Omar and A. A. Almhizia, *Chemosensors*, 2020, **8**, 86.



- 36 H. S. M. Abd-Rabboh, A. H. Kamel and A. E.-G. Amr, *Chemosensors*, 2020, **8**, 93.
- 37 A. G. Eldin, A. E.-G. E. Amr, A. H. Kamel and S. S. M. Hassan, *Molecules*, 2019, **24**, 1392.
- 38 A. H. Kamel and A. M. E. Hassan, *Int. J. Electrochem. Sci.*, 2016, **11**, 8938.
- 39 E. El-Naby and A. H. Kamel, *Mater. Sci. Eng., C*, 2015, **54**, 217.
- 40 A. M. El-Kosasy, A. H. Kamel, L. A. Hussin, M. F. Ayad and N. V. Fares, *Food Chem.*, 2018, **250**, 188.
- 41 A. H. Kamel, X. Jiang, P. Li and R. Liang, *Anal. Methods*, 2018, **10**, 3890.
- 42 A. H. Kamel, T. Y. Soror and F. M. Al Romian, *Anal. Methods*, 2012, **4**, 3007.
- 43 S. S. M. Hassan, I. H. A. Badr, A. H. Kamel and M. S. A. Mohamed, *Anal. Sci.*, 2009, **25**, 911.
- 44 A. H. Kamel and H. E. M. Sayour, *Electroanalysis*, 2009, **21**, 2701.
- 45 K. Koirala, F. B. Sevilla and J. H. Santos, *Sens. Actuators, B*, 2016, **222**, 391.
- 46 F. Tan, J. P. Metters and C. E. Banks, *Sens. Actuators, B*, 2013, **181**, 454.
- 47 N. B. Mincu, V. Lazar, D. Stan, C. M. Mihailescu, R. Iosub and A. L. Mateescu, *Diagnostics*, 2020, **10**, 517.
- 48 H. S. M. Abd-Rabboh, A. E. Amr, A. A. Almehizia and A. H. Kamel, *Polymers*, 2021, **13**, 1192.
- 49 E. Martínez-Periñán, C. Gutiérrez-Sánchez, T. García-Mendiola and E. Lorenzo, *Biosensors*, 2020, **10**, 118.
- 50 P. Shaikshavali, T. M. Reddy, V. N. Palakollu, R. Karpoormath, Y. S. Rao, G. Venkataprasad, T. V. Gopal and P. Gopal, *Synth. Met.*, 2019, **252**, 29.
- 51 P. Shaikshavali, T. M. Reddy, T. V. Gopal, G. Venkataprasad, V. S. Kotakadi, V. N. Palakollu and R. Karpoormath, *Colloids Surf., A*, 2020, **584**, 124038.
- 52 T. Guinovart, A. J. Bandodkar, J. R. Windmiller, J. R. Andrade and J. A. Wang, *Analyst*, 2013, **138**, 7031.
- 53 <https://pubchem.ncbi.nlm.nih.gov/compound/5311356>.
- 54 E. Bakker, *J. Electrochem. Soc.*, 1996, **143**, L83.
- 55 J. Bobacka, *Anal. Chem.*, 1999, **71**, 4932.

